

Origin of the large thermoelectric power in oxygen-variable  $R\text{BaCo}_2\text{O}_{5+x}$  ( $R=\text{Gd},\text{Nd}$ )A. A. Taskin,<sup>1</sup> A. N. Lavrov,<sup>2</sup> and Yoichi Ando<sup>1</sup><sup>1</sup>Central Research Institute of Electric Power Industry, Komae, Tokyo 201-8511, Japan<sup>2</sup>Institute of Inorganic Chemistry, Novosibirsk 630090, Russia

(Received 24 January 2006; published 6 March 2006)

Thermoelectric properties of  $\text{GdBaCo}_2\text{O}_{5+x}$  and  $\text{NdBaCo}_2\text{O}_{5+x}$  single crystals have been studied upon continuous doping of  $\text{CoO}_2$  planes with either electrons or holes. The thermoelectric response and the resistivity behavior reveal a hopping character of the transport in both compounds, providing the basis for understanding the recently found remarkable divergence of the Seebeck coefficient at  $x=0.5$ . The doping dependence of the thermoelectric power evinces that the configurational entropy of charge carriers, enhanced by their spin and orbital degeneracy, plays a key role in the origin of the large thermoelectric response in these correlated oxides.

DOI: 10.1103/PhysRevB.73.121101

PACS number(s): 72.20.Pa, 72.20.Ee, 72.80.Ga

Materials with strong electron-electron interactions, called strongly correlated electron systems, have recently attracted a great deal of attention as a promising alternative to conventional semiconductors in the field of thermoelectric power generation. The hope to find compounds with superior thermoelectric properties among correlated materials is based on the idea that in correlated systems, where the spin and orbital degrees of freedom play an important role in transport properties, the thermoelectric response can be enhanced by a large spin-orbital degeneracy of charge carriers.<sup>1-3</sup>

$\text{Na}_x\text{CoO}_2$  and several misfit-layered cobaltites with triangular-lattice  $\text{CoO}_2$  planes—materials demonstrating high thermoelectric response and metallic behavior<sup>4</sup>—have been considered as possible examples of compounds where the spin-orbital degeneracy plays a dominant role in enhancing the thermoelectric power.<sup>2,4</sup> However, a conventional Boltzmann-transport approach can also explain the coexistence of a large Seebeck coefficient and metallic conductivity in these compounds,<sup>5</sup> blurring the role and relevance of strong electron correlations.

Recently, layered cobaltites  $R\text{BaCo}_2\text{O}_{5+x}$  ( $R$  is a rare-earth element) with square-lattice  $\text{CoO}_2$  planes came into focus because of their remarkable transport and magnetic properties.<sup>6-8</sup> A variety of spin and orbital states are available in  $R\text{BaCo}_2\text{O}_{5+x}$  owing to its very rich phase diagram,<sup>8</sup> where  $x=0.5$  is the parent compound with all cobalt ions in the 3+ valence state. The variability of oxygen content in  $R\text{BaCo}_2\text{O}_{5+x}$  allows one to dope continuously the  $\text{CoO}_2$  planes with either electrons ( $\text{Co}^{2+}$  states) or holes ( $\text{Co}^{4+}$  states) and to measure a precise doping dependence of the Seebeck coefficient in one and the same crystal. Apart from this filling control, one can also employ a bandwidth control of transport properties using rare-earth elements  $R$  with different ionic radii [Fig. 1(a)] to clarify the role of band structure parameters in determining the thermoelectric power in these oxides. Thus,  $R\text{BaCo}_2\text{O}_{5+x}$  can provide a suitable ground for elucidating the relation between the spin-orbital degeneracy and thermoelectric properties in correlated materials.

Here we present a comparative study of the Seebeck coefficient and the resistivity in  $\text{GdBaCo}_2\text{O}_{5+x}$  (GBCO) and  $\text{NdBaCo}_2\text{O}_{5+x}$  (NBCO) single crystals over a wide range of electron and hole doping. Despite the difference in the lattice

parameters, both compounds show virtually the same behavior of the Seebeck coefficient, implying that the thermoelectric power in these compounds is governed by correlated hopping of charge carriers rather than the band structure parameters. An analysis of the doping dependence of the Seebeck coefficient, showing a spectacular divergence at  $x=0.5$ , provides evidence that the entropy contribution of charge carriers is the main source of the large thermoelectric power in  $R\text{BaCo}_2\text{O}_{5+x}$ .

High-quality  $\text{GdBaCo}_2\text{O}_{5+x}$  and  $\text{NdBaCo}_2\text{O}_{5+x}$  single crystals were grown using the floating-zone technique and their oxygen content was modified by high-temperature annealing treatments with subsequent quenching to room temperature.<sup>8</sup> Resistivity measurements were carried out by a standard ac four-probe method. The thermoelectric power was measured in a slowly oscillating thermal gradient of  $\sim 1$  K along the  $ab$  plane. The contribution from the gold wires ( $\sim 2$   $\mu\text{V}/\text{K}$ ) used as output leads was subtracted.

In parent  $R\text{BaCo}_2\text{O}_{5.5}$  compounds, the crystal lattice con-

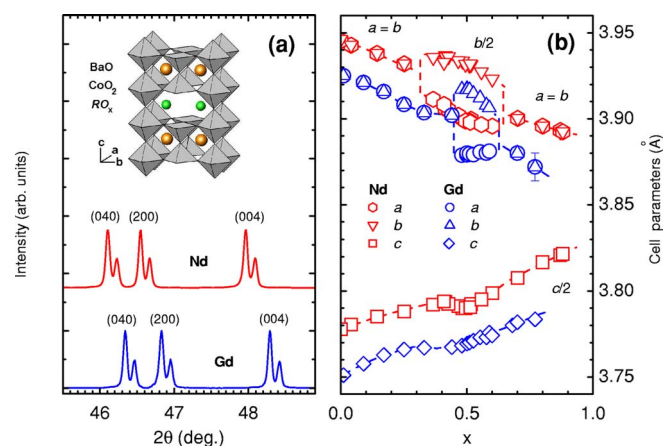


FIG. 1. (Color online) (a) X-ray Bragg peaks (200), (040), and (004), measured in  $\text{GdBaCo}_2\text{O}_{5.5}$  and  $\text{NdBaCo}_2\text{O}_{5.5}$  crystals at room temperature (each peak has  $\text{Cu } K\alpha_1$  and  $\text{Cu } K\alpha_2$  contributions to the diffraction pattern). Note that the unit cells are doubled along the  $b$  and  $c$  axes. A sketch of the crystal structure of  $R\text{BaCo}_2\text{O}_{5.5}$  is shown in the upper part of the panel. (b) The evolution of the room-temperature lattice parameters in  $\text{GdBaCo}_2\text{O}_{5+x}$  and  $\text{NdBaCo}_2\text{O}_{5+x}$  under variation of the oxygen content  $x$ .

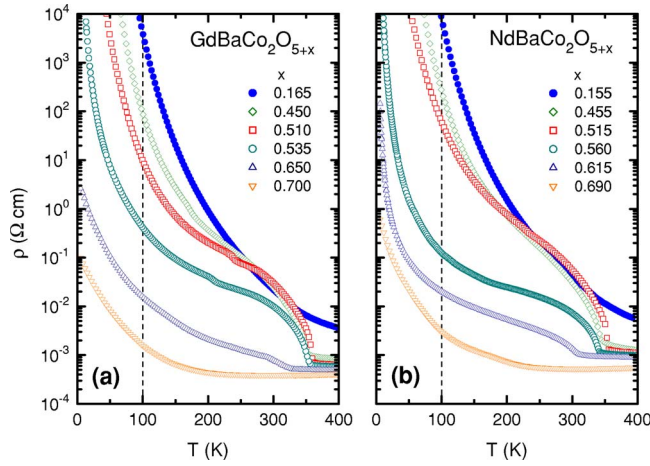


FIG. 2. (Color online) Temperature dependences of the in-plane resistivity  $\rho(T)$  of (a)  $\text{GdBaCo}_2\text{O}_{5+x}$  and (b)  $\text{NdBaCo}_2\text{O}_{5+x}$  crystals.

sists of equal numbers of  $\text{CoO}_6$  octahedra and  $\text{CoO}_5$  square pyramids [schematically shown in the inset of Fig. 1(a)]. Upon changing the oxygen content, some oxygen ions are inserted into or removed from the  $\text{RO}_x$  planes, which changes the number of  $\text{CoO}_6$  octahedra and  $\text{CoO}_5$  pyramids and also creates electrons or holes in  $\text{CoO}_2$  planes. Figure 1(b) shows the room-temperature lattice parameters in the entire available range of oxygen concentrations. Regardless of the oxygen content, the unit cell parameters in NBCO are found to be noticeably larger than in GBCO, in agreement with the larger ionic radius of Nd. This difference in the unit-cell size implies the difference in Co-O distances and/or O-Co-O angles, which determine the one-electron bandwidth; therefore, the substitution of the rare-earth element should affect the thermoelectric properties, if they are governed by the band structure parameters.

Figure 2 shows the temperature dependences of the resistivity in GBCO and NBCO for several oxygen concentrations. Both compounds demonstrate similar  $\rho(T)$  behavior, which strongly depends on the oxygen content. For oxygen concentrations close to the parent composition  $x=0.5$ ,  $\rho(T)$  curves show a sharp metal-insulator (MI) transition upon cooling below approximately the same temperature  $T_{MI} \approx 360$  K, while the MI transition seems to be smeared for  $x$  away from 0.5. Nevertheless, the low-temperature resistivity exhibits a hopping character for the entire range  $0 \leq x \leq 0.7$ , which allows us to consider the charge transport in terms of hopping of localized electrons ( $\text{Co}^{2+}$ ) or holes ( $\text{Co}^{4+}$ ). In the insulating regime, the resistivity in both compounds quickly decreases with hole doping, but remains unchanged or even increases with electron doping. This doping asymmetry can be explained by the different hopping probability of localized electrons ( $\text{Co}^{2+}$ ) and holes ( $\text{Co}^{4+}$ ) moving in the background of  $\text{Co}^{3+}$  ions because of the spin blockade of the electron transport.<sup>9</sup>

A comparison of the temperature dependences of the Seebeck coefficient  $Q(T)$  in GBCO and NBCO for several oxygen concentrations reveals a remarkable similarity of their thermoelectric properties (Fig. 3). Not only the temperature dependences are similar, but also the absolute values of  $Q(T)$

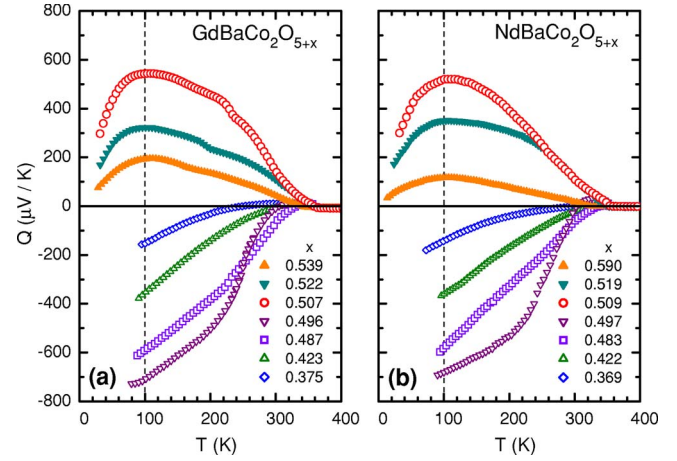


FIG. 3. (Color online) Temperature dependences of the Seebeck coefficient  $Q(T)$  of (a)  $\text{GdBaCo}_2\text{O}_{5+x}$  and (b)  $\text{NdBaCo}_2\text{O}_{5+x}$  crystals.

are virtually the same in GBCO and NBCO. At high temperatures, both compounds show a small, negative, and almost temperature-independent and doping-independent Seebeck coefficient, which is quite natural for a metallic state.<sup>8</sup> On the insulating side, on the other hand, the temperature dependences of the Seebeck coefficient are rather complicated and do not follow a simple  $\sim 1/T$  law expected for insulators.  $Q(T)$  depends strongly on the oxygen content, being negative for electrons and positive for holes, as shown in Fig. 4(a) for  $T=100$  K. Note that the absolute value of the Seebeck coefficient decreases rapidly upon doping with electrons or holes, in contrast to the asymmetric doping dependence of the conductivity, shown in Fig. 4(b) for the same temperature. The most striking feature in the doping dependence of the Seebeck coefficient  $Q(x)$  [Fig. 4(a)] is its remarkable divergence at  $x=0.5$ , where it reaches a large absolute value.

In order to clarify the origin of this large thermoelectric

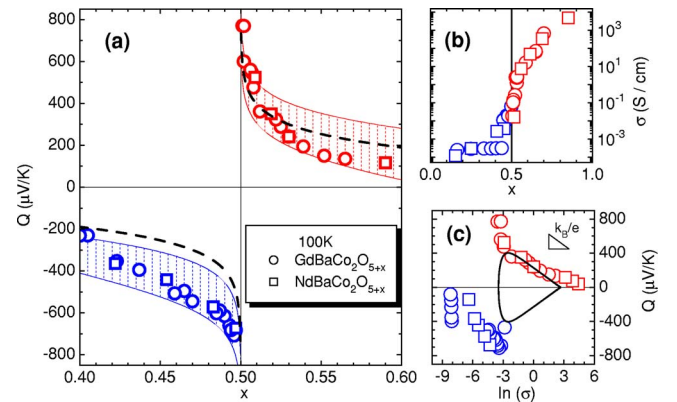


FIG. 4. (Color online) (a) The doping dependence of the Seebeck coefficient  $Q(x)$  of  $\text{GdBaCo}_2\text{O}_{5+x}$  (circles) and  $\text{NdBaCo}_2\text{O}_{5+x}$  (squares) crystals at  $T=100$  K. The hatched area represents the entire available range of the entropy contribution to the thermopower  $\Delta Q_n(x)$  and  $\Delta Q_p(x)$ . (b) The doping dependence of the conductivity  $\sigma(x)$  of  $\text{GdBaCo}_2\text{O}_{5+x}$  (circles) and  $\text{NdBaCo}_2\text{O}_{5+x}$  (squares) crystals at  $T=100$  K. (c) Jonker plot for  $\text{RBaCo}_2\text{O}_{5+x}$  (see text).

response, it is useful to consider what one would expect for the doping behavior if  $RBaCo_2O_{5+x}$  were an ordinary band gap material. Figure 4(c) shows the plot of  $Q$  versus the logarithm of the conductivity measured at  $T=100$  K—the so called Jonker plot.<sup>10</sup> For band gap materials, this plot is a curve with a universal shape [the pear-shaped curve, shown in Fig. 4(c)], which can be scaled by intrinsic parameters related to the energy band gap and scattering mechanism. In the extrinsic conduction region, the curve  $Q$  vs  $\ln(\sigma)$  has a slope  $\pm k_B/e$ , where  $k_B$  is the Boltzmann constant and  $e$  is the absolute value of the electron charge. Upon approaching the intrinsic-conduction region with decreasing concentration of electrons or holes, this slope can only decrease. As can be seen in Fig. 4(c), the actual slope of the Jonker plot for  $RBaCo_2O_{5+x}$  increases near the intrinsic conductivity region, exceeding the ideal  $k_B/e$  slope by several times. Moreover, the decrease of  $Q$  with electron doping does not correlate with the doping dependence of the conductivity, which shows no increase because of the spin blockade phenomenon.<sup>9</sup> Thus, both the temperature and doping dependences of the Seebeck coefficient clearly deviate from the behavior of conventional band gap materials.

Given the hopping character of the charge transport in  $RBaCo_2O_{5+x}$ , one can reasonably assume that a large part of the thermoelectric power comes from the entropy, which is carried by each electron or hole along with a charge. To check this assumption, let us examine the doping dependence of the Seebeck coefficient in GBCO and NBCO crystals,  $Q(x)$ , measured at  $T=100$  K [Fig. 4(a)]. Although the chosen temperature is presumably too low to achieve the true high-temperature limit, where the entropy contribution becomes the only contribution to the thermoelectric power,<sup>2</sup> it should be high enough to make reasonable estimations. Note that for  $RBaCo_2O_{5+x}$ , which undergoes a transition to a metallic state, the small and doping-independent Seebeck coefficient at high temperatures is governed by a different mechanism.<sup>8</sup>

The entropy contribution  $\Delta Q$  to the thermoelectric power in  $RBaCo_2O_{5+x}$  should be proportional to the change in the entropy  $S$  of the electron system upon introducing  $N$  charge carriers at constant internal energy  $E$  and volume  $V$  of the crystal,<sup>2</sup> where the entropy is determined by the total number of configurations  $\Omega$ , i.e., all possible arrangements of introduced carriers in the crystal lattice. Hence,  $\Delta Q$  is expressed in terms of  $\Omega$  as

$$\Delta Q = -\frac{1}{e} \left( \frac{\partial S}{\partial N} \right)_{E,V} = -\frac{k_B}{e} \frac{\partial \ln \Omega}{\partial N}. \quad (1)$$

Thus, the description of the doping dependence of the Seebeck coefficient  $Q(x)$  in our case can be reduced to a combinatorial problem.

In the simplest case of nondegenerate carriers, the above approach gives the celebrated Heikes formula<sup>1</sup>

$$\Delta Q_n = -\frac{k_B}{e} \ln \left[ \frac{\frac{1}{2} + x}{\frac{1}{2} - x} \right], \quad \Delta Q_p = \frac{k_B}{e} \ln \left[ \frac{\frac{3}{2} - x}{x - \frac{1}{2}} \right]. \quad (2)$$

Both electron  $\Delta Q_n$  and hole  $\Delta Q_p$  contributions are shown in Fig. 4(a) by the dashed lines. A comparison with experimental data shows that this simple model, albeit it gives a rough

idea of why the Seebeck coefficient can diverge at  $x=0.5$ , is not sufficient for a quantitative description of the doping dependence  $Q(x)$  in  $RBaCo_2O_{5+x}$ , especially in the case of electron doping.

As has been recently emphasized by Koshibae and Maekawa,<sup>2</sup> the spin-orbital degeneracy of charge carriers plays an important role in systems with correlated hopping transport. In  $RBaCo_2O_{5+x}$ , there are two kinds of lattice sites for cobalt ions that differ in the local oxygen environment [see the inset of Fig. 1(a)], namely,  $x$  octahedra and  $(1-x)$  pyramids, which provide different spin-orbital states for introduced electrons ( $Co^{2+}$ ), holes ( $Co^{4+}$ ), or host  $Co^{3+}$  ions. For electron doping, if one knows the distribution of introduced electrons ( $Co^{2+}$ ) between octahedral and pyramidal positions, the total number of configurations  $\Omega$  is determined by

$$\Omega = g_{2o}^{N_{2o}} g_{2p}^{N_{2p}} g_{3o}^{N_{3o}} g_{3p}^{N_{3p}} \cdot \frac{N_L!}{N_{2o}! N_{2p}! N_{3o}! N_{3p}!}, \quad (3)$$

where  $N_L$  is the total number of cobalt sites;  $N_{2o}$  and  $N_{2p}$  ( $N_{3o}$  and  $N_{3p}$ ) are the numbers of  $Co^{2+}$  ( $Co^{3+}$ ) ions in octahedral and pyramidal positions, respectively;  $g_{2o}$ ,  $g_{2p}$ ,  $g_{3o}$ , and  $g_{3p}$  are the degeneracies of these states. An analogous expression can be written for hole doping as well.

At any given doping level in the range of  $0 \leq x \leq \frac{1}{2}$ , the equilibrium concentrations of  $Co^{2+}$  and  $Co^{3+}$  ions in different positions are determined by the only parameter—a probability  $p$  to find a  $Co^{2+}$  ion in an octahedral position. For  $x$  close to  $x=0.5$ , where the number of doped carries is not large, this probability is determined by the law of mass action  $(N_{2p}N_{3o})/(N_{2o}N_{3p})=K(T)$ ,<sup>11</sup> which couples the equilibrium concentrations of  $Co^{2+}$  and  $Co^{3+}$  ions that are competing for octahedral and pyramidal positions. This equation can be analytically solved for  $p$ , yielding

$$p = \frac{\sqrt{\left(\frac{K+1}{2}\right)^2 + 4(K-1) \cdot \left(\frac{1}{2} - x\right)} x - \frac{K+1}{2}}{2(K-1) \left(\frac{1}{2} - x\right)}, \quad (4)$$

where  $K(T)$  is the equilibrium constant, which depends only on the temperature and intrinsic characteristics of the system, such as the difference in energies of  $Co^{2+}$  (and  $Co^{3+}$ ) ions in octahedral and pyramidal positions.

Using Eqs. (1), (3), and (4), the analytical solution for the entropy contribution of doped electrons to the thermoelectric power can be written as follows:

$$\Delta Q_n = -\frac{k_B}{e} \ln \left[ \frac{g_{2o}^m g_{2p}^{1-m}}{g_{3o}^{1+m} g_{3p}^{-m}} \cdot \frac{N_{3o}^{1+m} N_{3p}^{-m}}{N_{2o}^m N_{2p}^{1-m}} \right], \quad (5)$$

where  $m \equiv p + (x - \frac{1}{2}) \partial p / \partial x$ . Upon electron doping,  $m$  can change its value in the range from  $-1$  to  $+1$ , depending on the intrinsic characteristics of the system. The entropy contribution of doped holes to the thermoelectric power in the range  $\frac{1}{2} \leq x \leq 1$  can be obtained in the same way.

As follows from Eq. (5), there are only two factors that affect the doping dependence of the Seebeck coefficient: The equilibrium constant  $K$ , which determines the occupation of

octahedral (pyramidal) positions by doped electrons, and degeneracies of states  $g_i$ , which turn out to be the main source of the thermoelectric-power enhancement in  $R\text{BaCo}_2\text{O}_{5+x}$  near  $x=0.5$ . Note that the entropy contribution to the thermoelectric power is expected to be insensitive to the unit-cell size, which gives a natural account for the similarity of the Seebeck coefficient  $Q(T)$  in GBCO and NBCO.

It is well known that owing to a comparable strength of the exchange interaction and the crystal field splitting,  $\text{Co}^{3+}$  ions can adopt different spin states, depending on the oxygen environment or even on temperature.<sup>12</sup> It is believed that in the parent  $R\text{BaCo}_2\text{O}_{5.5}$  at low temperature, the  $\text{Co}^{3+}$  ions adopt the low-spin (LS) state in octahedra and the intermediate-spin (IS) state in pyramids.<sup>7,8</sup> For  $\text{Co}^{2+}$  the crystal field is weaker than for  $\text{Co}^{3+}$  and thus  $\text{Co}^{2+}$  adopts the high-spin (HS) state, while for  $\text{Co}^{4+}$  the crystal field is stronger, favoring the LS state. Any state with nonzero spin  $S$  has the degeneracy  $2S+1$ . In addition to this spin degeneracy, there can be orbital degeneracy as well. For both  $\text{HS-Co}^{2+}$  and  $\text{LS-Co}^{4+}$  the orbital state is threefold degenerate because of a hole residing in the  $t_{2g}$  orbitals. In general, the orbital degeneracy can be lifted by lowering the crystal symmetry. For a rough estimation, we assume that the orbital degeneracy in pyramidal positions is lifted, which gives the following spin-orbital degeneracies:  $g_{2o}=12$ ,  $g_{2p}=4$ ,  $g_{3o}=1$ ,  $g_{3p}=3$ ,  $g_{4o}=6$ , and  $g_{4p}=2$ .

The hatched area in Fig. 4(a) shows the entire available range of  $\Delta Q_n(x)$  and  $\Delta Q_p(x)$  for  $R\text{BaCo}_2\text{O}_{5+x}$ , which is obtained by changing the equilibrium constant  $K$  from one extreme to another (where  $p$  changes from 0 to 1) and keeping the spin-orbital degeneracies unchanged. As can be seen in Fig. 4(a), all experimental values of the Seebeck coefficient lie within this area. This gives confidence that the entropy contribution of charge carriers, which includes their spin-orbital degeneracy, can account for the doping dependence of the Seebeck coefficient and its remarkable divergence at  $x=0.5$ . Also, this model naturally accounts for the somewhat enhanced thermoelectric response in electron-doped crystals in comparison with the hole-doped ones: The larger Seebeck coefficient for electrons can be explained by the larger degeneracy of  $\text{HS-Co}^{2+}$  in comparison with  $\text{LS-Co}^{4+}$ .

In conclusion, the present study of thermoelectric and transport properties in  $R\text{BaCo}_2\text{O}_{5+x}$  gives a solid experimental support to the idea that strong electron correlations and spin-orbital degeneracy can bring about a large thermoelectric power in transition-metal oxides.

<sup>1</sup>P. M. Chaikin and G. Beni, Phys. Rev. B **13**, 647 (1976).

<sup>2</sup>W. Koshibae, K. Tsutsui, and S. Maekawa, Phys. Rev. B **62**, 6869 (2000); W. Koshibae and S. Maekawa, Phys. Rev. Lett. **87**, 236603 (2001).

<sup>3</sup>V. S. Oudovenko and G. Kotliar, Phys. Rev. B **65**, 075102 (2002).

<sup>4</sup>I. Terasaki, Y. Sasago, and K. Uchinokura, Phys. Rev. B **56**, R12685 (1997); Y. Ando, N. Miyamoto, K. Segawa, T. Kawata and I. Terasaki, *ibid.* **60**, 10580 (1999); Y. Wang, N. S. Rogado, R. J. Cava, and N. P. Ong, Nature (London) **423**, 425 (2003).

<sup>5</sup>D. J. Singh, Phys. Rev. B **61**, 13397 (2000); T. Takeuchi, T. Kondo, T. Takami, H. Takahashi, H. Ikuta, U. Mizutani, K. Soda, R. Funahashi, M. Shikano, M. Mikami, S. Tsuda, T. Yokoya, S. Shin, and T. Muro, *ibid.* **69**, 125410 (2004).

<sup>6</sup>C. Martin, A. Maignan, D. Pelloquin, N. Nguyen, and B. Raveau,

Appl. Phys. Lett. **71**, 1421 (1997).

<sup>7</sup>M. Respaud, C. Frontera, J. L. García-Muñoz, Miguel Angel G. Aranda, B. Raquet, J. M. Broto, H. Rakoto, M. Goiran, A. Llobet, and J. Rodríguez-Carvajal, Phys. Rev. B **64**, 214401 (2001).

<sup>8</sup>A. A. Taskin, A. N. Lavrov, and Y. Ando, Phys. Rev. B **71**, 134414 (2005).

<sup>9</sup>A. Maignan, V. Caignaert, B. Raveau, D. Khomskii, and G. Sawatzky, Phys. Rev. Lett. **93**, 026401 (2004); A. A. Taskin and Y. Ando, *ibid.* **95**, 176603 (2005).

<sup>10</sup>G. H. Jonker, Philips Res. Rep. **23**, 131 (1968); G. M. Choi, H. L. Tuller, and D. Goldschmidt, Phys. Rev. B **34**, 6972 (1986).

<sup>11</sup>F. A. Kröger, *The Chemistry of Imperfect Crystals* (North-Holland, Amsterdam, 1974).

<sup>12</sup>P. M. Raccach and J. B. Goodenough, Phys. Rev. **155**, 932 (1967).